

Cover Page



Universiteit Leiden



The handle <http://hdl.handle.net/1887/19036> holds various files of this Leiden University dissertation.

Author: Bommel, Rutger Jan van

Title: Cardiac resynchronization therapy : determinants of patient outcome and emerging indications

Issue Date: 2012-05-31

Chapter 4

Analysis of ventricular activation using surface electrocardiography to predict left ventricular reverse volumetric remodeling during cardiac resynchronization therapy

Sweeney MO, **van Bommel RJ**, Schalij MJ, Borleffs CJ, Hellkamp AS, Bax JJ

Circulation 2010;121(5):626-34

ABSTRACT

Background: Cardiac resynchronization therapy (CRT) for heart failure with left bundle branch block (LBBB) reduces left ventricular (LV) conduction delay, contraction asynchrony and LV end-systolic volume (ESV, "remodeling"). Up to 1/3 of patients do not improve and the electrical requirements for remodeling are unclear. We hypothesized that remodeling is predicted by the LBBB ventricular activation sequence, the paced activation sequence and interactions between these 2 conditions.

Methods: 12-lead ECGs during LBBB and CRT were analyzed in 202 consecutive patients (NYHA Class III-IV heart failure, ejection fraction $\leq 35\%$) for predictors of remodeling ($\geq 10\%$ reduction in ESV) at 6 months.

Results: Greater baseline LV activation time (LVAT_{max}) predicted increased odds of remodeling (OR[CI] = 1.30 [1.11, 1.52] per 10 ms increase), whereas higher QRS Scores for LV scar predicted reduced remodeling (OR[CI] = 0.49 [0.27, 0.88] for each 1 point increase from 0 - 4; 0.92 [0.83, 1.01] for each 1 point >4). Post-CRT, increasing R amplitudes in leads V1-V2 (OR[CI] = 2.76 [1.01, 7.51] for each 1X increase over [baseline R X 4.5]), and left \rightarrow right frontal axis shift (OR[CI] = 2.00 [0.99, 4.02]), indicators of ventricular activation wavefront fusion, were positive predictors of remodeling. Predicted probability of remodeling ranged from $<20\%$ for patients with adverse predictors to 99% for those with positive predictors.

Conclusions: Ventricular activation using the ECG accurately predicts LV remodeling during CRT. Greater baseline LVAT_{max} and smaller scar volume combined with wavefront fusion on the paced ECG, anticipate higher probability of remodeling.

INTRODUCTION

Left ventricular (LV) conduction delay due to left bundle branch block (LBBB) causes regional heterogeneity in contraction and stretch (asynchrony) which reduces pump function and stimulates negative LV remodeling. The conceptual basis of cardiac resynchronization therapy (CRT) is to minimize LV conduction delay, which reduces contractile asynchrony and instantaneously improves LV mechanics.^{1,2} Resynchronization of electromechanical activation induces “reverse” remodeling (LV volume reductions) and improved pump function (increased LV ejection fraction, LVEF).^{3,4}

The requisite conditions during which reversal of LV conduction delay result in remodeling are unknown. We hypothesized that the volumetric remodeling response to CRT can be predicted by the baseline LBBB ventricular activation sequence, the paced ventricular activation sequence and the interaction between these 2 conditions.

METHODS

We developed a predictive model to test the hypothesis that the probability of reverse volumetric remodeling could be accurately characterized by the ventricular activation pattern on the 12-lead surface ECG before and after CRT.

Study sample

The study sample consisted of 202 consecutive patients with NYHA Class III-IV heart failure despite medical therapy, LVEF $\leq 35\%$, and LBBB (QRS duration (QRSd) ≥ 120 ms; delayed intrinsic deflection in leads I, V5, V6 ≥ 50 ms; broad slurred R waves in I, aVL, V5 and V6; rS or QS waves in V1 -V2; ST-T-wave vectors opposite the major QRS vector). Patients with right bundle branch block (RBBB), right ventricular (RV) pacing, or myocardial infarction ≤ 3 months prior were excluded. Simultaneous BV pacing was applied without exception for the first 6 months.

Echocardiography and electrocardiography

Standard supine 12-lead ECGs (filter range, 0.15 to 100 Hz; AC filter, 60 Hz, 25 mm/s, 10 mm/mV) were obtained at baseline and pre-discharge. Echocardiograms were performed at baseline and after 6 months of CRT. Patients were imaged in the left lateral decubitus position with a commercially available system (Vingmed System Seven, General Electric-Vingmed, Milwaukee, Wisconsin, USA) using a 3.5-MHz transducer at a depth of 16 cm in conventional

parasternal and apical views. Standard 2-dimensional and color Doppler data triggered to the QRS complex were saved in cine-loop format. ESV and end-diastolic volume (EDV) were measured at the apical 2- and 4-chamber views; LVEF was calculated using the biplane Simpson's method.⁵ Inter- and intra-observer variability for LV volume measures were 90% and 96%, respectively.⁶

ECG analysis of ventricular activation

ECGs were analyzed blinded to echocardiographic results. All measurements were made using digital calipers at 200% magnification calibrated for paper speed 25 mm/second. Normal frontal plane axis was $+90^\circ \leftrightarrow <-30^\circ$, left axis deviation (LADEV) $\geq -30^\circ \leftrightarrow <-60^\circ$, right axis deviation (RADEV) $\geq -90^\circ \leftrightarrow >+90^\circ$. Right superior axis (RSA) was $>180^\circ \leftrightarrow -90^\circ$; right inferior axis (RIA) $+90^\circ \leftrightarrow 180^\circ$. "Incomplete" right superior axis (IRSA) was defined as extreme LADEV ($-60^\circ \leftrightarrow -90^\circ$) with rS or QS complexes in the inferior leads and equiphasic QR in I (see below for QRS hieroglyphic framework). Axis quadrant shift was defined as displacement of LBBB frontal plane axis by ≥ 1 quadrant during CRT (i.e., normal \rightarrow LADEV, normal \rightarrow RSA).

QRS hieroglyphic framework for ventricular activation pattern comparisons

The QRS complex in each lead pre- and post-CRT was deconstructed into 4 possible waveform elements (R, S, Q, QS). Absolute amplitudes (mV) and durations (ms) of all elements of each QRS complex were used to characterize specific activation patterns (i.e., R and S present, $R > S$ amplitude, pattern = Rs) Ventricular activation in each lead was characterized by 9 possible patterns, or QRS hieroglyphs: (1) R, (2) RS ($R=S$ and both >1 mm, or both <1 mm; equiphasic), (3) Rs ($R > s$), (4) rS ($S > r$), (5) QS, (6) qR ($q < R$), (7) QR ($Q=R >1$ mm, or both <1 mm; equiphasic), (8) Qr ($Q > r$), (9) QRS (all 3 waveforms present).

Characterization of ventricular activation during LBBB

Typical LBBB activation is registered as right (R) \rightarrow left (L) (frontal plane), anterior (A) \rightarrow posterior (P) (horizontal plane), and variable axis. This yields a QRS hieroglyphic signature with dominant positive forces in I, aVL (R, Rs), negative forces in aVR (QS), variable forces in II, III, AVF (R, Rs, rS, QS), dominant negative forces in V1-V2 (QS, rS), transition V3-V5 (rS \rightarrow Rs, R) and dominant positive forces in V5-V6 (R, Rs).

QRS notching

LBBB is characterized by sequential ventricular activation (RV → LV)^{2, 7-9} and registered as fragmented QRS complexes with RSR' configuration ("notch"). QRS notching was defined as ≥1 notch in the R or S wave present in ≥2 adjacent anterior, lateral or inferior leads.¹⁰

RV and LV activation time

Because multiple notches in the R and S wave during LBBB may occur due to myocardial scar,¹⁰ the first notch was assumed to indicate the transition between RV and LV depolarization. Notching in the first 40 ms of the S wave in V1-V2 was excluded since this indicates scar in the QRS score. RV activation time (RVAT) was measured as time (ms) between QRS onset and first notch in any of ≥2 adjacent leads. LV activation time (LVAT) was QRSd - RVAT (ms).

For modeling purposes, the longest LVAT (LVAT_{max}) recorded in any lead and region was used. A numerical relationship between QRSd and LVAT_{max} was derived using linear regression [LVAT_{max} (ms) = -35.839 + 0.763*QRSd (ms) + 0.000619*QRSd (ms)²], permitting estimation of LVAT_{max} in the absence of QRS notching (40 patients).

Quantification of LV scar

Myocardial scar has been linked to reduced CRT response.¹¹ ECG quantification of LV scar volume was calculated using the Selvester QRS score for LBBB.¹² The effects of scar on LBBB surface registration translate as specific QRS hieroglyphic signatures, manifest as unopposed rightward electrical forces by infarct region: qR, QR, rS in I, aVL (anterior-superior); qR, QR, rS in I, V5-V6 (apical); qR, QR, rS in II, aVF (inferior); QS → rS, RS, or Rs in V1-V2 (anterior-septal). Posterior-lateral infarct does not have a specific QRS hieroglyphic signature but is included in the QRS score.

Evidence for ventricular activation fusion during BV pacing

Experimental models of LBBB demonstrate maximum improvement in LV pump function occurs when intra-LV electrical asynchrony is minimized by wavefront fusion.² Wavefront opposition and reversal during BV pacing should yield ECG-evidence of fusion:

- (1) Expected change in frontal plane electrical axis: normal or LADEV → RADEV

(2) Expected changes in QRS hieroglyphic signatures: Rightward forces emerge in leads with dominant leftward forces (R in I, aVL → qR, QR, QS). Anterior forces emerge in leads with dominant posterior forces (QS in V1 → rS, RS, Rs, R; QS or rS in V2 → RS, Rs, R; rS or RS V3 → Rs or R, etc).

(3) Expected directional change in regional or global mean of R wave amplitudes

Though LV pacing yields specific ventricular activation patterns generally in accordance with stimulation site, nearly identical ECG activation sequences may be registered at widely spaced sites,¹³ and electrical resynchronization during CRT correlates unpredictably with stimulation site due to conduction blocks.⁹ For these reasons, LV lead position was not relevant to this analysis.

End-points

The primary end-point was LV reverse volumetric remodeling, defined as $\geq 10\%$ reduction in ESV at 6 months.⁴ Supplemental remodeling end-points, chosen to provide additional insights into the predictive model were, $\geq 10\%$ reduction in EDV (mechanistically similar measure of remodeling) and $\geq 30\%$ reduction in ESV ("superresponse").⁴

Statistical analysis

For descriptive summaries, categorical variables are presented as N (%), and continuous variables as median (25th, 75th percentile).

Indices of change in R amplitude were generated by calculating, for each patient, the change in R amplitude for each lead from baseline to post-CRT, as a proportion of the baseline value. The post-implant value was used where an R was absent at baseline and present post-implant; a value of 1 used where an R was present at baseline and absent post-implant; and a value of 0 used where both were absent. Change values were set to positive if the change was in the expected direction (decrease in I, aVL, and V4-V6; increase in V1-V3); negative otherwise. Leads II, III, and aVF had no expected direction and retained their calculated sign. These change values were then averaged across relevant leads for each patient. Four summaries were created: (1) mean of I and aVL; (2) mean of V1 and V2; (3) mean of all leads except aVR; and (4) mean of I, aVL, V1-V6.

Candidate predictors for multivariable modeling were selected using the framework describe above, including variables that characterize LBBB (LVAT, LV scar volume, QRS hieroglyphs) and expected evidence of ventricular fusion (axis change, change in R amplitudes,

and changes in QRS hieroglyphic signatures). Where several related measures were available (e.g., regional LVAT vs. $LVAT_{max}$), univariate tests were used to determine which measure had the strongest relationship with the end-point. Continuous variables were checked for linearity of their relationship with the outcome, and revised versions (usually truncations) created where necessary; and categorical variables related to each other were checked to determine if a combination of the variables would be a better predictor than the individual variables.

After this screening process, 13 variables were selected as candidates for the primary end-point logistic regression model (6 baseline, 7 post-CRT). Baseline variables were: QRSd, $LVAT_{max}$, QRS score, QS hieroglyph in aVR, R hieroglyph in V6, and R >5 mV in V5 or V6. Post-CRT variables were: LADEV → RADEV, R → Qr, qR, QR, or QS in I and aVL, new R waves >5 mV in both V1 and V2, and mean change in R amplitude in the expected direction in I and aVL, V1 and V2, and in all leads except aVR. For the 2 supplemental models, the same set of predictors was used, with minor modifications.

For each end-point, all candidate predictors were entered into a logistic regression model, and stepwise selection then used to identify the set of significant independent predictors. Relative risk is expressed as odds ratio (95% confidence interval) (OR[CI]). Predicted probabilities of the primary end-point were generated from the final logistic regression model. Where model variables are not specifically displayed in a plot, median or mode values were used in generating predictions (QRS points = 6, change in R amplitude = 4.5, LADEV → RADEV = no). For characterizing tiers of response, patients were divided into low, middle, and high responders, with predicted probability of response = 0-49%, 50-74%, and 75-100%, respectively, and patterns among their predictor values examined.

RESULTS

The median (25th, 75th percentile) age was 67 (60, 75) years. Overall, 73% were male and 53% had an ischemic cardiomyopathy. $LVAT_{max}$ was approximately 2/3 QRSd and longest in the inferior leads. On average, about 20% of the LV volume was scar. CRT resulted in a slight reduction in median QRSd, overall rightward frontal plane axis shift, modest reductions in ESV and EDV, and modest increases in LVEF (Table 1).

Table 1. Echocardiographic and electrocardiographic variables at baseline and post CRT

Variable	
Baseline	
<i>Echocardiographic measurements</i>	
ESV (ml)	157 (116-199)
EDV (ml)	207 (163-252)
LVEF (%)	25 (19-30)
<i>Electrocardiographic measurements</i>	
Atrial fibrillation	23 (11%)
QRS duration (ms)	165 (148-176)
Frontal plane axis (degrees)	-31 (-51--8.0)
LADEV	98 (49%)
LVAT (ms)	
Inferior	109 (90-130)
Lateral	100 (81-116)
Anterior	103 (93-129)
Maximum any region	113 (93-129)
QRS score	
Total QRS score points	6.0 (4.0-9.0)
% LV scar from QRS score	18 (12-27)
Post CRT	
<i>Echocardiographic measurements</i>	
ESV (ml)	124 (88-167)
EDV (ml)	183 (140-230)
LVEF (%)	32 (26-38)
<i>Electrocardiographic measurements</i>	
Atrial fibrillation	14 (7%)
QRS duration (ms)	158 (142-174)
Frontal plane axis (degrees)	-99 (-121--76)
LADEV	35 (17%)

n = 202 patients. Continuous variables are shown as median (25th, 75th percentile)

QRS hieroglyphs by pivotal leads: baseline and post-CRT

The preliminary screening process for candidate predictors of $\geq 10\%$ reduction in ESV indicated that the expected changes in local and regional QRS hieroglyphic signatures were most pronounced in I, aVL, V1 and V2, which were designated pivotal leads. During LBBB, a dominant L \rightarrow R, A \rightarrow P activation pattern was observed in $\geq 95\%$ of patients (Table 2). Less than 5% of patients had R \rightarrow L and/or P \rightarrow A activation, due to dominant Q or S waves in I and aVL and R waves in V1-V2, caused by scar.

During CRT, rightward forces emerged in I and aVL and anterior forces in leads V1-V2. These effects were greatest in I and V1, and were observed in 74% and 53% of patients, respectively. Reciprocally, evidence of persistent leftward and posterior activation was recorded in 26% (I) and 47% (V1) of patients during CRT.

Table 2. QRS hieroglyphs by pivotal leads at baseline and post CRT

Surface lead	Baseline	Post CRT
I	Dominant leftward	Dominant rightward/equiphasic
	R, Rs	QS
	qR	rS, Qr, QR, RS
	Dominant rightward/equiphasic	Dominant leftward
	QS, rS, Qr, RS, QR	R, Rs, qR
aVL	Dominant leftward	Dominant rightward/equiphasic
	R, Rs	QS
	qR	rS, Qr, QR, RS
	Dominant rightward/equiphasic	Dominant leftward
	QS, rS, Qr, QR	R, Rs, qR, QRS
V1	Dominant posterior	Dominant anterior/equiphasic
	rS	R, Rs, qR
	QS	RS, QRS
	Dominant rightward/equiphasic	Dominant leftward
	Rs, qR, QRS, Qr	QS, rS
V2	Dominant posterior	Dominant rightward/equiphasic
	rS	R, Rs, qR
	QS	RS, QRS, QR
	Dominant rightward/equiphasic	Dominant leftward
	Rs, Qr, RS	QS, rS, Qr

Evidence for ventricular activation fusion during CRT

A rightward axis emerged in 67% of patients during CRT. However, a RSA was observed in only 58% and RIA in 9%. In contrast, 20% had LADEV or normal axis during CRT, and 12% had IRSA. Therefore, nearly 1/3 of patients did not have evidence of ventricular fusion by frontal plane axis during CRT. Similarly, though $\approx 90\%$ had an axis quadrant shift during CRT, a RSA or RIA was achieved in only 3/4 of these patients. The remaining 1/4 had primarily a leftward (LADEV or IRSA) axis quadrant shift.

Evidence for ventricular fusion using QRS hieroglyphs was recorded in all 4 pivotal leads with greatest frequency in I and V1. Evidence of wavefront collision (Q and S emergence, R regression) was observed in I for 71% of patients. However, total (QS) or near-total (Qr) reversal of activation in I was observed in only 55%. Similarly, total reversal of activation in V1 (dominant R emergence) was observed in only 50%. Evidence for activation reversal was $\approx 50\%$ less evident in aVL and V2.

A $\geq 50\%$ reduction in R wave amplitude in I and aVL, reflecting L \leftrightarrow R wavefront fusion in the horizontal plane, was observed in 60% of patients. Reciprocally, a $\geq 50\%$ increase in R wave amplitude in V1 and V2, due to A \leftrightarrow P wavefront fusion, was observed in only 62%.

Table 3. Evidence for ventricular activation fusion during simultaneous biventricular pacing

Frontal plane electrical axis	
Median absolute axis change (degrees)	85 (47-131)
RADEV	136 (67.7%)
RSA	118 (58.4%)
RIA	18 (8.9%)
IRSA	25 (12.4%)
LADEV	35 (17.3%)
Normal axis	6 (3.0%)
Axis quadrant shift	180 (89.1%)
Rightward: Normal/LADEV → RADEV	134 (66.3%)
RSA	116 (57.4%)
RIA	18 (8.9%)
Incomplete rightward: Normal/LADEV → IRSA	25 (12.4%)
Leftward: Normal → LADEV	16 (7.9%)
Other	5 (2.5%)
Activation wavefront reversal in pivotal leads	
I: Q emergence, S emergence, R regression	144 (71.3%)
R, Rs, rS, RS → QS	104 (51.5%)
R, Rs, rS, RS → Qr	8 (4.0%)
R, Rs, rS, RS → qR	21 (10.4%)
R, Rs, rS, RS → QR	11 (5.4%)
aVL: Q emergence, S emergence, R regression	59 (29.2%)
R, Rs, rS, RS → QS	27 (13.4%)
R, Rs, rS, RS → Qr	4 (2.0%)
R, Rs, rS, RS → qR	24 (11.9%)
R, Rs, rS, RS → QR	4 (2.0%)
V1: R emergence, QS regression	
QS or rS → R, Rs, RS	100 (49.5%)
V2: R emergence, QS or rS regression	
QS or rS → R, Rs, RS	48 (23.8%)
Mean R amplitude change ≥50% in expected direction for pivotal leads	
I and aVL	121 (59.9%)
V1 and V2	100 (49.5%)

Predictors of ≥ 10% reduction in ESV at 6 months

A multivariable model identified 2 baseline and 2 post-CRT independent predictors of ≥10% reduction in ESV at 6 months (Table 4). Increasing $LVAT_{max}$ was associated with a greater probability of ≥10% reduction in ESV (OR[CI] = 1.30 [1.11, 1.52] per 10 ms increase) up to 125 ms; for longer $LVAT_{max}$ there was no further increase in probability of response (Figure 1). Patients with values in the lowest quartile (≤ 80 ms) had a 51% response rate compared to 73% response in patients with values of ≥ 125 ms or longer. Though QRSd was weakly as-

Table 4. Multivariate model for predictors of $\geq 10\%$ reduction in end-systolic volume

Variable	Odds ratio (95%CI) for ESV reduction	p-value
Baseline		
LVAT _{max}	1.30 (1.11-1.52) for each 10 ms increase up to 125	0.0010
QRS score	0.49 (0.27-0.88) for each 1 point increase from 0 to 4	0.0022*
	0.92 (0.83-1.01) for each 1 point increase >4	
Post CRT		
Mean change in R amplitude in V1 and V2 in expected direction	2.76 (1.01, 7.51) for each 1 mV increase >4.5	0.048
LADEV to RADEV	2.00 (0.99, 4.02)	0.052

Model c-index = 0.74

*Overall test

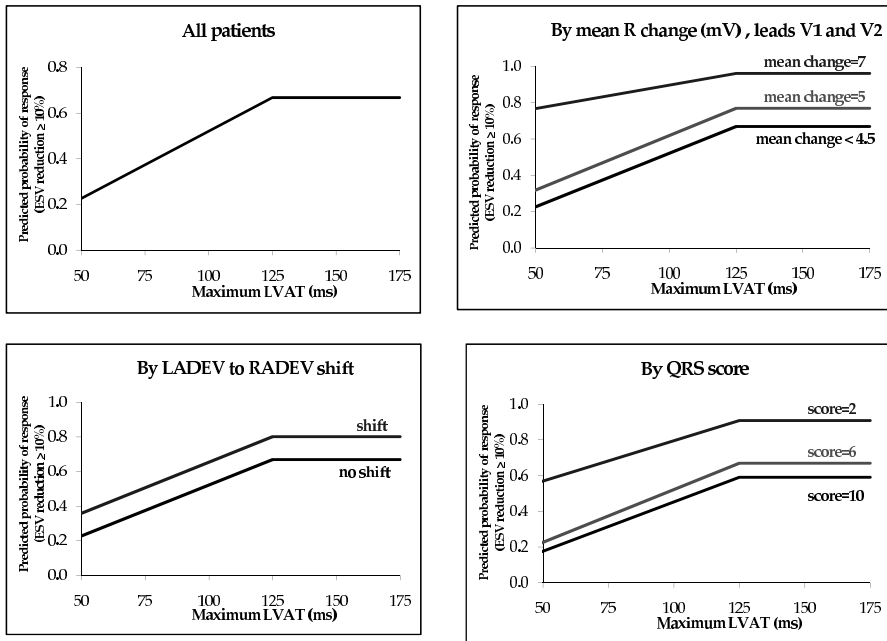


Figure 1. Probability of reverse remodeling by baseline and post CRT predictors.

sociated with remodeling probability in preliminary univariate comparisons, this relationship was replaced by $LVAT_{max}$ in the multivariable model.

Increasing QRS scores were negatively associated with reverse remodeling (OR[CI] = 0.49 [0.27, 0.88] for each 1 point increase from 0 to 4; 0.92 [0.83, 1.01] for each 1 point increase above 4). Patients with QRS scores in the lowest quartile (0-3) had a response rate of 78% compared to patients with scores in the highest quartile (>9), whose response rate was 45%.

Post-CRT, increasing R amplitudes in V1-V2, indicating ventricular fusion, were associated with increased probability of reverse remodeling. This effect was not observed until the mean change in R amplitude was $\geq 4.5x$ the baseline value (OR[CI] = 2.76 [1.01, 7.51] for each 1x increase $\geq 4.5x$). Although only 25 patients fell in this upper range, the response rate was 84% vs. 60% in patients with mean change V1-V2 R $< 4.5x$ baseline. A second measure of ventricular fusion, LADEV \rightarrow RADEV, was associated with increased probability of reverse remodeling (OR[CI] = 2.00 [0.99, 4.02]). Patients showing this axis quadrant shift had a response rate of 70% compared to 60% in patients without.

Visual evidence for the effect of $LVAT_{max}$ and the other independent predictors of reverse remodeling is provided in Figure 1. Predicted probability of remodeling is greatest for longer baseline $LVAT_{max}$ in the presence of post-CRT ventricular fusion, indicated by larger changes in R amplitude in leads V1-V2 (top right) and LADEV \rightarrow RADEV axis quadrant shift (lower left). In contrast, the positive effects of increasing $LVAT_{max}$ are offset by higher QRS scores such that longer $LVAT_{max}$ in the presence of a high QRS score has lower predicted probability of remodeling than very short $LVAT_{max}$ in the presence of a low QRS score (lower right).

Predicting reverse remodeling using a global measure of ventricular fusion

An alternate way of characterizing evidence for ventricular fusion is using a measure of change in R wave amplitude in the expected direction in lateral (I, aVL) and precordial (V1-V6) leads (CHRLP) before and after CRT (Figure 2). As for most of the amplitude change variables, there was no change in probability of remodeling for the lowest values. Probability of remodeling did not start to increase with larger CHRLP until post-CRT values were greater than baseline ((OR(CI) = 3.14 (0.97, 10.15) for each 1x increased above 1, $p = 0.056$), whereas all patients with CHRLP < 1 had equivalent probability of response, regardless of the actual CHRLP value.

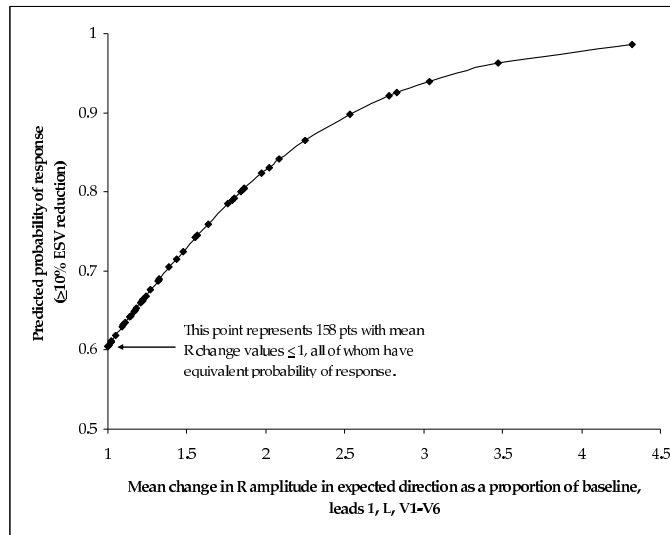


Figure 2. Predicting reverse remodeling using a global measure of ventricular fusion.

Tiers of reverse remodeling response

Response tiers are shown in Table 5. The multivariable predictive model showed good discrimination, with a c-index of 0.70. Low responders had ≥ 1 adverse value for baseline predictors (i.e., QRS score >17 , $LVAT_{max} < 60$ ms), or offsetting combinations (i.e., QRS score 3-5 + $LVAT_{max} \leq 90$ ms, or $LVAT_{max} > 110$ ms + QRS score ≥ 12), or mid-range values (i.e., $LVAT_{max}$ 90-110 ms, QRS score 6-11). Very short $LVAT_{max}$ (48-62 ms) occurred only in this group and no QRS scores 0-2. These patients also had limited or absent fusion evidence post-CRT (Figure 3).

High responders had ≥ 1 favorable predictors (i.e., QRS score < 3 , or change in R amplitude > 5), or a combinations of favorable predictors (i.e., QRS score 3 and $LVAT_{max} > 110$ ms, or QRS score 4-9, $LVAT_{max} > 110$ ms and quadrant shift). Alternately, high responders had fair values for 1 predictor that were offset by very favorable values for others (i.e., smaller change in R amplitude but $LVAT_{max} > 130$ ms). There were no QRS scores > 12 whereas all changes in R amplitude > 5 occurred in the high responders (Figure 3).

Middle range responders had intermediate values for predictors (i.e., $LVAT_{max}$ 90-110 ms, QRS score 6-11, quadrant shift, mid-range change in R amplitude), or an offsetting combination of vary favorable and mid-range predictor values (i.e., long $LVAT_{max}$ but high QRS score and small change in R amplitude)

Table 5. Predicted probabilities of low, middle and high responders

<i>Tier</i>	<i>n</i>	<i>Range of predicted probability (%)</i>	<i>Mean predicted probability (%)</i>	<i>Actual response rate (%)</i>
Low response	56	0% to <50%	39%	41%
Middle response	88	50% to <75%	63%	61%
High response	58	75% to 100%	88%	88%

Predictors of supplemental reverse remodeling end-points

Multivariable models for supplemental remodeling end-points yielded similar predictors as the $\geq 10\%$ ESV reduction model (Table 6). The $\geq 30\%$ ESV reduction end-point was met by 59 (29.2%) patients. Each 10 ms increase in $LVAT_{max}$ was associated with increased probability of $\geq 30\%$ ESV reduction, slightly less vs. the $\geq 10\%$ ESV model (OR = 1.23 vs. 1.30). The relationship of QRS score, for its entire range, to a $\geq 30\%$ reduction in ESV was similar to the relationship of QRS score above 4 to a $\geq 10\%$ reduction in ESV (OR = 0.91 vs. 0.92 for each 1 point increase). Ventricular fusion (V2 R amplitude change from <1 to >5 mm) also predicted $\geq 30\%$ ESV reduction (OR = 2.90). Axis quadrant shift was not significant, possibly due to the lower event rate.

The $\geq 10\%$ EDV reduction end-point was met by 45.5% (92/202) patients. Greater $LVAT_{max}$ was directly associated with EDV reduction (OR = 1.92 for each 10 ms increase up to 95) whereas higher QRS scores were inversely related (OR = 0.87 for each 1 point increase). Ventricular fusion (V1 R amplitude change from <1 to >5 mm) also predicted EDV reduction (OR = 3.03); axis quadrant shift did not.

Table 6. Multivariate predictors of supplemental remodeling end-points

<i>Variable</i>	<i>Reverse remodeling end-point</i>	<i>p-value</i>
	ESV odds ratio (95% CI) for $\geq 30\%$ reduction*	
Baseline		
$LVAT_{max}$	1.23 (1.09-1.40) for each 10 ms increase	0.0013
QRS score	0.91 (0.82-0.99) for each 1 point increase	0.045
Post CRT		
Baseline V2 R $<1 \rightarrow$ Post V2 R >5	2.90 (1.30-6.45)	0.0090
	EDV odds ratio (95% CI) for $\geq 10\%$ reduction*	
Baseline		
$LVAT_{max}$	1.92 (1.34-2.76) for each 10 ms increase up to 95	0.0004
QRS score	0.87 (0.80, 0.95) for each 1 point increase	0.0019
Post CRT		
Baseline V1 R $<1 \rightarrow$ Post V1 R >5	3.03 (1.17-7.82)	0.022

*Model c-index 0.70 for both ESV and EDV

DISCUSSION

This study demonstrates that the probability of reverse volumetric LV remodeling during CRT in patients with asynchronous heart failure and LBBB can be accurately predicted by characterization of the ventricular activation sequence before and after CRT using the standard 12-lead ECG. The main findings are that: (1) the translational mechanism for volumetric remodeling is activation wavefront fusion, which is evident on the paced ECG, and (2) the probability of remodeling is positively influenced by LV conduction delay ($LVAT_{max}$) and negatively influenced by LV scar volume (QRS score) on the baseline ECG.

Uncertainty regarding the physiology of ventricular resynchronization is reflected in significant heterogeneity in clinical response to CRT. A CRT responder feels better, has less heart failure morbidity, and demonstrates evidence of reverse remodeling; a non-responder exhibits none of these. Up to 1/3 of CRT patients are non-responders.^{14, 15} The reasons for this are complex and incompletely characterized but most likely relate to poorly understood interactions between substrate conditions and pacing-induced changes in ventricular activation.

We evaluated reverse volumetric remodeling as an end-point because (1) experimental models have demonstrated a direct linkage between LV electrical activation, mechanics and remodeling,^{2, 16} (2) remodeling is associated with reduced heart failure morbidity and mortality,⁴ and (3) it is the least subjective element of CRT response.

At baseline, longer $LVAT_{max}$ was significantly associated with ESV reduction, indicating that greater LV conduction delay is associated with higher probability of reverse remodeling assuming delay is sufficiently corrected by CRT. In contrast, each QRS score point (indicative of 3% LV scar volume) was associated with a reduction in the probability of reverse remodeling, with the greatest effect in the lower points range (0-4). Higher LV scar volume is associated with lower probability of reverse remodeling. Post-CRT, larger changes in R wave amplitude in pivotal leads V1-V2, indicating P → A activation reversal, and LADEV → RADEV frontal plane axis quadrant shift, indicating L → R activation reversal, were associated with an increased probability of reverse remodeling. Higher CHRLP scores, a global measure of change in ventricular activation during CRT, also predicted ESV reduction. Therefore, paced ventricular activation wavefront fusion increases the probability of reverse remodeling. These results provide evidence that interactions between myocardial substrate (scar volume), baseline LV conduction delay, and paced-activation wavefronts (fusion response) anticipate the probability of reverse remodeling. These results were duplicated in multivariable models for supplemental remodeling end-points ($\geq 30\%$ reduction in ESV and $\geq 10\%$ reduction in EDV).

This study provides a framework for understanding the heterogeneous clinical response to CRT. The interaction between substrate conditions, post-CRT evidence of ventricular fusion, and the probability of reverse remodeling is evident in the characterization of low, middle and high probability responders. Patients with small $LVAT_{max}$ and large LV scar volume are unlikely

to remodel even when paced fusion is present (“volumetric nonresponders”). “Volumetric superresponders” are characterized by large conduction delays, small scar volumes and the most robust evidence of paced fusion. Several other observations regarding the interaction between substrate conditions and post-CRT evidence of ventricular fusion are evident in Figure 1. At very high values of $LVAT_{max}$ the probability of remodeling was still at least 40-50% even for weak or absent paced ECG evidence for ventricular fusion (i.e., no LADEV → RADEV axis quadrant shift or low range increases in V1-V2 R amplitudes). Reciprocally, for very low values of $LVAT_{max}$ the probability of remodeling may still reach 80% if there is strong paced ECG evidence for ventricular fusion (i.e., highest range increases in V1-V2 R amplitudes).

Only 2/3 of patients had paced ECG evidence of ventricular fusion. This implies that failure to correct LV conduction delay, despite BV pacing, contributes significantly to volumetric non-response. Nearly 20% of patients had axis quadrant shift to LADEV or IRSA (extreme LADEV) and 10% had a normal axis during CRT. In some of these patients, failure to generate ECG evidence of fusion during simultaneous BV pacing was likely due to LV capture latency, conduction delay or blocks^{8,9} with a common consequence of different bidirectional paced activation times favoring persistent R → L, A → P conduction. Sequential BV pacing might improve the fusion response in some of these patients, especially the subset with IRSA. It is also likely that fusion failure in some patients was due to stimulation from a site incapable of reversing LV activation.

On the other hand, the probability of volumetric remodeling was reasonably high in some patients even without paced ECG evidence of ventricular fusion. Global ventricular activation patterns are represented by the 12-lead ECG whereas local activation patterns may be concealed.⁹ Reduction of local conduction delay sufficient to improve regional LV mechanics may be concealed within the surface registration of the paced ECG; alternately concealed local activation patterns may prevent LV electrical resynchronization. Since the translation of cardiac electrical activation to the surface ECG is incompletely understood, interpretation of ventricular activation using any surface method may be unpredictably incorrect.

This study supports the concept that asynchronous heart failure is fundamentally an electrical disorder than can be resolved at the level of ventricular conduction. A close linkage between electrical and mechanical asynchrony has been demonstrated in animal models¹⁷ and preliminarily in humans.¹⁸ The greater the LV conduction delay, the greater the potential gains in remodeling when conduction delay is sufficiently corrected, assuming LV scar volume is not prohibitive. Targeting LV pacing sites using real-time ECGs to evaluate evidence of activation wavefront fusion and reversal, rather than rigid adherence to anatomic targets, may improve CRT response.

Limitations

Echocardiographic measures of LV volumes may be less accurate than other methods. The surface ECG may not accurately reflect important changes in LV activation. QRS score is modestly less accurate than newer imaging methods for calculating scar volume.

Conclusions

Ventricular activation on the surface ECG accurately predicts ventricular remodeling during CRT. Greater $LVAT_{max}$ and smaller scar volume on the baseline LBBB ECG, combined with wavefront fusion on the paced ECG, are associated with higher probability of ESV reduction.

REFERENCES

1. Auricchio A, Stellbrink C, Block M et al. Effect of pacing chamber and atrioventricular delay on acute systolic function of paced patients with congestive heart failure. The Pacing Therapies for Congestive Heart Failure Study Group. The Guidant Congestive Heart Failure Research Group. *Circulation* 1999;99:2993-3001.
2. Verbeek XA, Vernooy K, Peschar M. Intra-ventricular resynchronization for optimal left ventricular function during pacing in experimental left bundle branch block. *J Am Coll Cardiol* 2003;42:558-567.
3. St John Sutton MG, Plappert T, Abraham WT et al. Effect of cardiac resynchronization therapy on left ventricular size and function in chronic heart failure. *Circulation* 2003;105:1985-1990.
4. Ypenburg C, van Bommel RJ, Borleffs CJW et al. Long-term prognosis after cardiac resynchronization therapy is related to the extent of left ventricular reverse remodeling at midterm follow-up. *J Am Coll Cardiol* 2009;53:483-490.
5. Schiller NB, Shah PM, Crawford M et al. Recommendations for quantification of the left ventricle by two-dimensional echocardiography. *J Am Soc Echocardiogr* 1989;2:358-367.
6. Ypenburg C, Roes SD, Bleeker GB et al. Effect of total scar burden on contrast-enhanced magnetic resonance imaging on response to cardiac resynchronization therapy. *Am J Cardiol* 2007;99:657-660.
7. Rodriguez LM, Timmermans C, Nabar A, Beatty G, Wellens HJ. Variable patterns of septal activation in patients with left bundle branch block. *J Cardiovasc Electrophysiol* 2003;14:135-141.
8. Auricchio A, Fantoni C, Regoli F et al. Characterization of left ventricular activation in patients with heart failure and left bundle branch block. *Circulation* 2004;109:1133-1139.
9. Jia P, Ramanathan C, Ghanem RN, Kyungmoo R, Varma N, Rudy Y. Electrocardiographic imaging of cardiac resynchronization therapy in heart failure: Observation of variable electrophysiologic responses. *Heart Rhythm* 2006;3:296-310.
10. Das MK, Suradi H, Maskoun W et al. Fragmented Wide QRS on a 12-Lead ECG: A Sign of Myocardial Scar and Poor Prognosis. *Circ Arrhythmia Electrophysiol* 2008;1:258-268.
11. White JA, Yee R, Yuan X et al. Delayed enhancement magnetic resonance imaging predicts response to cardiac resynchronization therapy in patients with intraventricular dyssynchrony. *J Am Coll Cardiol* 2006;48:1953-1960.
12. Strauss DG, Selvester RH, Lima JAC et al. ECG quantification of myocardial scar in cardiomyopathy patients with or without conduction defects: correlation with cardiac magnetic resonance and arrhythmogenesis. *Circ Arrhythmia Electrophysiol* 2008;1:327-336.
13. Giudici MC, Tigrett DW, Carlson JI, Lorenz TD, Paul DL, Barold SS. Electrocardiographic patterns during pacing the great cardiac and middle cardiac veins. *Pacing and Clinical Electrophysiology* 2007;30:1376-1380.
14. Abraham WT, Fisher WG, Smith AL et al. Cardiac resynchronization in chronic heart failure. *N Eng J Med* 2002;346:1845-1853.
15. Bax JJ, Marwick TH, Molhoek SG et al. Left ventricular dyssynchrony predicts benefit of cardiac resynchronization therapy in patients with end-stage heart failure before pacemaker implantation. *Am J Cardiol*. 2003;92:1238-1240.
16. Vernooy K, Cornelussen RNM, Verbeek XAAM et al. Cardiac resynchronization therapy cures dyssynchronopathy in canine left bundle-branch block hearts. *Eur Heart J* 2007;28:2148-2155.

17. Wyman BT, Hunter WC, Prinzen FW, Farris OP, McVeigh ER. Effects of single- and biventricular pacing on temporal and spatial dynamics of ventricular contraction. *Am J Physiol* 2002;282:H372-H379.
18. Ghosh S, Avari JN, Canham RM et al. Concordance between left ventricular electrical and mechanical synchrony in nonischemic patients undergoing cardiac resynchronization therapy. *Heart Rhythm* 2009;6:S127.